

# Three-dimensional reconstruction of Haversian systems in human cortical bone using synchrotron radiation-based micro-CT: morphology and quantification of branching and transverse connections across age

Isabel S. Maggiano,<sup>1,2</sup> Corey M. Maggiano,<sup>2,3</sup> John G. Clement,<sup>4</sup> C. David L. Thomas,<sup>4</sup> Yasmin Carter<sup>5</sup> and David M. L. Cooper<sup>1</sup>

<sup>1</sup>Department of Anatomy and Cell Biology, University of Saskatchewan, Saskatoon, SK, Canada

<sup>2</sup>Department of Anthropology, University of West Georgia, Carrollton, GA, USA

<sup>3</sup>Department of Anthropology, University of Western Ontario, London, ON, Canada

<sup>4</sup>Melbourne Dental School, University of Melbourne, Melbourne, Vic., Australia

<sup>5</sup>Department of Radiology, University of Massachusetts Medical School, Worcester, MA, USA

---

## Abstract

This study uses synchrotron radiation-based micro-computed tomography (CT) scans to reconstruct three-dimensional networks of Haversian systems in human cortical bone in order to observe and analyse interconnectivity of Haversian systems and the development of total Haversian networks across different ages. A better knowledge of how Haversian systems interact with each other is essential to improve understanding of remodeling mechanisms and bone maintenance; however, previous methodological approaches (e.g. serial sections) did not reveal enough detail to follow the specific morphology of Haversian branching, for example. Accordingly, the aim of the present study was to identify the morphological diversity of branching patterns and transverse connections, and to understand how they change with age. Two types of branching morphologies were identified: lateral branching, resulting in small osteon branches bifurcating off of larger Haversian canals; and dichotomous branching, the formation of two new osteonal branches from one. The reconstructions in this study also suggest that Haversian systems frequently target previously existing systems as a path for their course, resulting in a cross-sectional morphology frequently referred to as 'type II osteons'. Transverse connections were diverse in their course from linear to oblique to curvy. Quantitative assessment of age-related trends indicates that while in younger human individuals transverse connections were most common, in older individuals more evidence of connections resulting from Haversian systems growing inside previously existing systems was found. Despite these changes in morphological characteristics, a relatively constant degree of overall interconnectivity is maintained throughout life. Altogether, the present study reveals important details about Haversian systems and their relation to each other that can be used towards a better understanding of cortical bone remodeling as well as a more accurate interpretation of morphological variants of osteons in cross-sectional microscopy. Permitting visibility of reversal lines, synchrotron radiation-based micro-CT is a valuable tool for the reconstruction of Haversian systems, and future analyses have the potential to further improve understanding of various important aspects of bone growth, maintenance and health.

**Key words:** age; branching; cortical bone; Haversian system; micro-CT; osteon; synchrotron; three-dimensional.

---

## Correspondence

Isabel S. Maggiano, Anthropology Department, West Georgia University, 1601 Maple Street, Carrollton, GA, 30118, E: [imaggian@westga.edu](mailto:imaggian@westga.edu)

Accepted for publication 19 November 2015

## Introduction

Human cortical bone has a dynamic and complex microstructure that is maintained and renewed continuously throughout life by two different processes, 'modeling' and 'remodeling'. While modeling causes changes in a

bone's net volume, as bone is added or removed, remodeling describes the replacement of previously existing tissue. Remodeling rates change with age and in response to physical activity; about 5% of cortical bone is removed and replaced each year in adults (Martin et al. 1998). Understanding basic remodeling processes and functions is necessary to understand various aspects of bone growth and health, including osteoporosis, and is intimately linked to knowledge of its resulting microstructure. Moreover, bone microstructural interpretations are important in any investigation of bone; anatomical, biomedical or anthropological. They have been gainfully employed towards age estimation of unknown individuals (Kerley, 1965; Stout, 1988) and investigations of disease pathogenesis alike (Schultz, 2001).

Remodeling results in structural units called Haversian systems. The formation of Haversian systems is accomplished by basic multicellular units (BMUs), the coordinated activity of osteoclasts (bone-resorbing cells) and osteoblasts (bone-forming cells; Frost, 1963, 1969). It consists of three consecutive phases: resorption, reversal and formation. During the resorption phase, osteoclasts form a tunnel or cutting cone through previously existing mineralized bone tissue, leaving evidence of their activity in Howship's lacunae, pits formed from bursts of resorptive activity by individual osteoclasts. The combined effect of many osteoclasts creates the roughened reversal line, which in transverse two-dimensional (2D) histology is visible as a scalloped edge. Osteoblasts appear in the reversal phase and initiate formation, through sequential mineralization of proteins they secrete, called osteoid. During this process, they first form the cement line, emphasized by localized irregularity of the osteoid matrix as it is deposited on the roughened, previously resorptive surface (Skedros et al. 2005). The combined effect of the microstructural disruption and increased mineral density in this region becomes visible as a darkened ring surrounding the osteon in optical microscopy of thin ground sections. Once this cement line has formed, the cavity is successively filled by lamellae, until only the Haversian canal is left. While some remodeling is non-targeted or stochastic, other turn-over targets active or microdamaged regions permitting mechanical adaptation, self-repair and preventing degradation (Ortner, 1975; Burr, 1993; Schaffler et al. 1995; Martin, 2002, 2007; Parfitt, 2002).

In 2D studies, 'secondary osteons', or type I osteons, are characterized as roughly circular in cross-section, about 250  $\mu\text{m}$  in diameter. From the three-dimensional (3D) perspective, Haversian systems in human cortical bone are long (often  $> 1$  cm), irregularly cylindrical structures (Hennig et al. 2015). Studies of resorption cavities in human cortical bone show a potential for variable morphologies of Haversian systems from interconnected or clustered to branched. Resorption cavities have been shown to run unidirectional or simultaneously in two or more directions through several

branches (Schumacher, 1935; Cohen & Harris, 1958; Vasca-veo & Bartoli, 1961; Johnson, 1964; Tappen, 1977; Cooper et al. 2003, 2004, 2006; Basillais et al. 2004; Matsumoto et al. 2005; Schneider et al. 2007; Britz et al. 2012; Carter et al. 2013, 2014). Accordingly, the 3D reality of Haversian systems is quite complex; they are both branched and connected through transversely oriented canals, building complex, dynamic networks (Koltze, 1951; Cohen & Harris, 1958; Stout et al. 1999; Cooper et al. 2011).

Until now, 3D reconstructions of Haversian networks have been demonstrated on exemplary samples of one individual each by Cooper et al. [2011; using synchrotron radiation-based micro-computed tomography (CT) scans] and Arhatari et al. (2011; using phase retrieval tomography). Haversian system interconnection and branching morphology is inaccessible utilizing more common optical techniques, even those involving laborious serial sectioning, which, due to the thickness of the sections, do not typically resolve enough detail. However, some other approaches, as for example analyses of resorption spaces or canal networks (Tappen, 1977; Cooper et al. 2003, 2006) and analyses of stained vessel networks in non-human animals (Pazzaglia et al. 2007, 2011) have added valuable information. Three-dimensional reconstructions are an important additional tool for creating a better understanding of Haversian systems, their interconnections, and their interactions with surrounding bone tissue as well as age-related changes of total Haversian networks.

Part of the reason for age effects seen in changing osteonal morphology is likely connected to maturation and maintenance of bone vasculature, which is directly linked to remodeling. In addition to this maintenance, vasculature is necessary for BMU activity (both nutrient supply and cell recruitment; Brookes & Revell, 1998; Pazzaglia et al. 2011). The vascular network in human cortical bone is characterized by a predominantly longitudinal lattice through primary canals in periosteal bone. Endosteal bone, however, shows a transversely oriented pattern connecting cortical bone with the marrow cavity (Enlow, 1963; Maggiano, 2012). Secondarily remodeled regions of bone are characterized by a 'ladder-like' lattice, longitudinally oriented vessels running through Haversian systems connected through transversely oriented canals. Despite differing influences on and functions for the BMU, the net result of remodeling is that the accumulation of Haversian systems is fairly regular on the whole. However, the specific regional distribution of osteons has been shown to vary considerably across diaphyseal cross-sections, emphasizing the complexity of remodeling and bone growth and adaptation (McFarlin et al. 2008; Goldman et al. 2009; Maggiano et al. 2011, 2015; Pazzaglia et al. 2013; Maggiano, 2015).

Synchrotron radiation-based micro-CT scans have been shown to be useful for the reconstruction of Haversian networks (Cooper et al. 2011; Arhatari et al. 2011 for the employment of phase retrieval tomography). Using this

approach, the present study reconstructs human Haversian networks from the mid-diaphyseal femur of individuals of different ages in order to: (i) describe the morphological variability of branching events and transverse connections; (ii) quantify all branching events and transverse connections within the sampled volumes; and (iii) identify age-related trends of Haversian system branching and interconnectivity.

## Materials and methods

Femora used in this study are part of the Melbourne Femur Collection held at the University of Melbourne, Australia. As a component of a larger study, samples of 36 men between the ages of 18 and 92 years were collected during autopsy with the informed consent of the donor's next-of-kin. All individuals had no known conditions that may have affected their bones. The study was conducted with ethical approval from the Victorian Institute of Forensic Medicine (EC26/2000), the University of Melbourne (HREC 980139) and the University of Saskatchewan (Bio # 08-46). Of each bone, a rectilinear sample with dimensions of  $\sim 2 \times 2 \times 5$  mm was cut from the anterior mid-cortex of the proximal femoral shaft. A sub-sample of six specimens with diverse ages (20, 27, 39, 46, 62, 71 years) was included in the present study.

Synchrotron radiation-based micro-CT scanning was conducted at the Advanced Photon Source (APS), Argonne National Laboratory, IL, USA, on beamline 2BM. Projection images were obtained using monochromatic x-rays with a photon energy of 27.9 keV and an effective pixel size of 1.47  $\mu\text{m}$ . Raw data collection involved the capture of 1800 frames spanning 180 degrees of rotation in a scan time of approximately 9 min. The projection images were reconstructed to create a 3D dataset ( $2016 \times 2016 \times 900$  voxels).

Images were analysed utilizing imaging software AMIRA 5.4.1. (Visage Imaging, Berlin, Germany). A Gaussian smoothing filter was applied performing a convolution operation. The size of the convolution kernel was chosen at  $3 \times 3 \times 10$  at 0.8 sigma along all axes. Using these image parameters osteon boundaries became even more visible, owing to their unique mineral quality and/or collagen-influenced morphology (Fig. 1). Unfortunately, the comparably

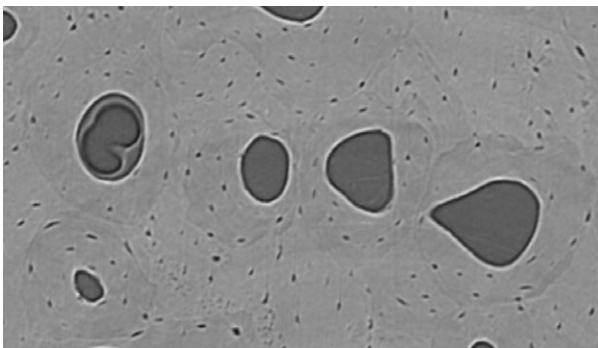


**Fig. 1** Synchrotron micro-CT scanning creates a cross-sectional view of several osteons under digital zoom. Reversal lines were traced on each 10th slice, with all slices available for interpretation of changing morphology along the z-axis. If reversal lines were slightly obscured in one image, their morphology could be easily determined by altering the viewing perspective up and down along the volume's depth (z-dimension).

smaller and more homogenous interfaces between individual lamellae (or lamellar pairs) remained obscured, limiting direct observation of osteonal morphology to the external surface (at the reversal line) and internal surface (at the Haversian canal). The complex morphology of Haversian systems could be reconstructed manually by hand-outlining the reversal lines, even where they appeared within Haversian systems or as a branching segment between two or more systems. Manual tracing was performed on every 10th z-axis slice through the imaged volume (roughly 90 tracings out of the total 899 slices, capturing a 2D representation of 3D morphology every 14.5  $\mu\text{m}$ ). To provide data between outlines interpolations were generated and inspected for the rare occasions where additional manual adjustments were necessary. For best visualization, each Haversian system was saved separately and data were resampled to decrease the total image size. During this process, four pixels were averaged in each dimension, thus the resulting 3D renders were created with an isotropic voxel size of 5.88  $\mu\text{m}^3$ . Canals and void spaces were visualized using threshold-driven segmentation (Cooper et al. 2011).

A 2D, squared region of interest ( $1.5 \times 1.5$  mm) with the highest prevalence of osteons was selected on the fifth slice of each sample (slices 1–5 and 895–899 were excluded from the sample, due to decreased visibility of osteon boundaries). All osteons with cross-sectional areas of at least 50% within this region of interest were included in the study regardless of their continuous course along the z-axis. The z-axis was 1.3 mm long, resulting in a reconstructed volume of  $1.5 \times 1.5 \times 1.3$  mm ( $2.925$  mm<sup>3</sup>).

Continuous remodeling and branching forms a complex network of Haversian systems characterized by a high degree of interconnectivity (Fig. 2). Haversian systems are frequently interrupted by branching, interception and other interactions between two systems, creating segments of diverse lengths. In the following these segments are referred to as 'osteonal segments'. All osteonal segments together are part of a continuum, the total Haversian network. Because osteonal segments are objectively confineable, they represent useful tools for the analysis of total Haversian networks in three dimensions, in the same way osteons and fragments have served analytical and histomorphometric purposes through optical microscopy of thin ground sections. In the present study, they were used as quantifiable units. The following characteristics confine osteonal segments: (i) nodes formed by branching or interception events; (ii) interruption of previously existing systems by relatively younger systems; and (iii) 'blindly' ending osteonal segments. All interconnections confining osteonal segments and all connections along their longitudinal course were quantified (interactions of osteonal segments with systems from outside the region of interest were also included) in order to follow trends characterizing Haversian interconnectivity across age. Because of the relatively small sample size used in this study, a limitation caused by the time-consuming nature of outlining reversal lines by hand, quantitative trends were observed without statistical testing.

## Results

### The 3D morphology of Haversian branching

Haversian branching can be separated into different types, according to morphological distinctions observed in this study. To name and describe them, general terminology for branching morphologies in other biological systems is borrowed.

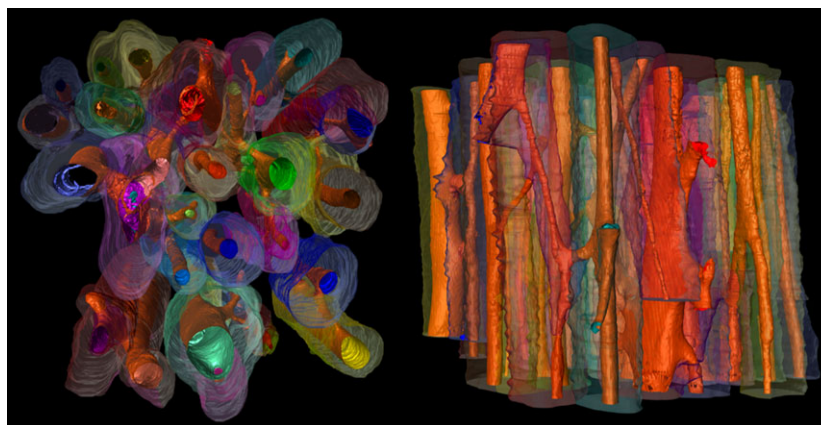


**Fig. 2** Haversian network reconstruction (2.925 mm<sup>3</sup>). Synchrotron micro-CT images analysed in Amira 5.4.1., visualizing the 3D morphological complexity of the Haversian network. Image generated through: (i) systematically hand-drawn reversal lines from z-axis images reconstructing the osteonal morphology with interpolated outlines between the manual outlines (multi-hued); and (ii) automated recognition of canals and void spaces (in orange).

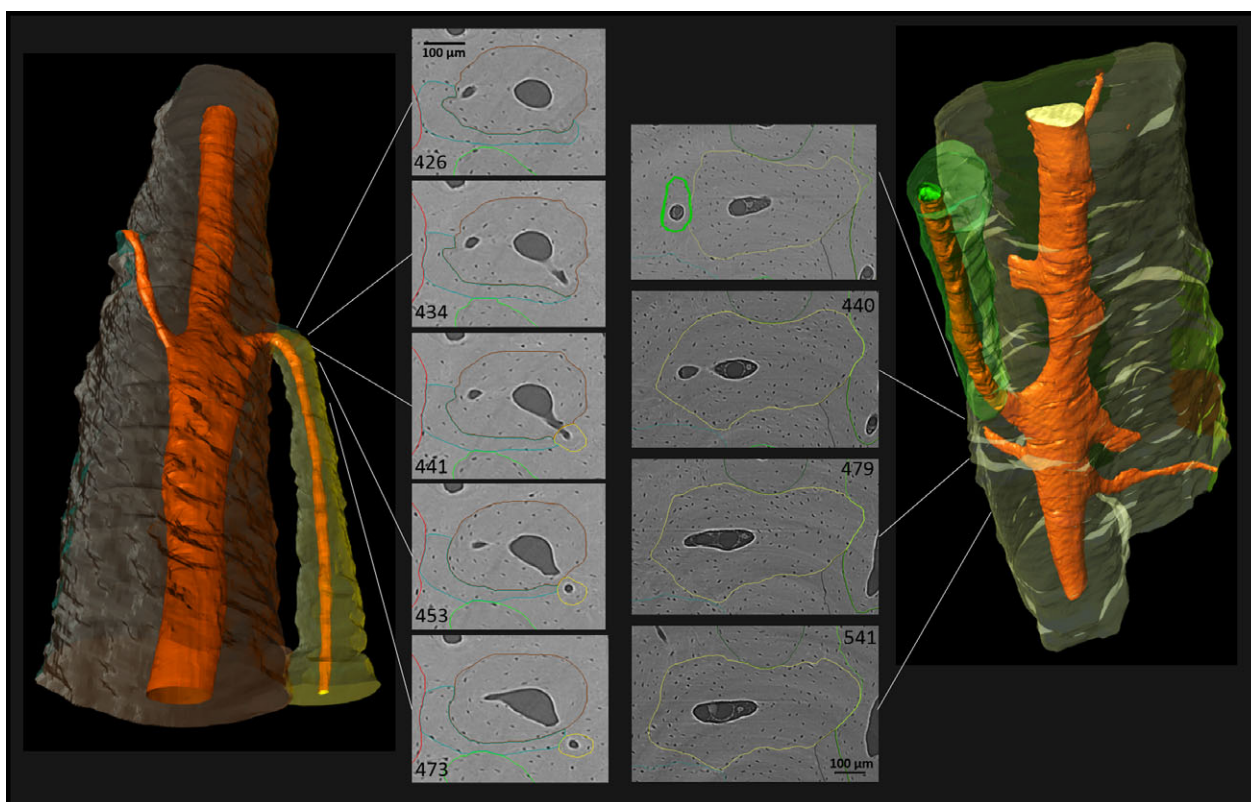


**Fig. 3** Lateral branching characterized by a newly formed canal that connects the Haversian canal of a previously existing Haversian system with adjacent tissue, where it extends through the formation of a new BMU. Note the consistency in cross-sectional size and shape of the previously existing system, the almost perpendicular angle of the newly formed canal, especially in the left example, and the size difference between the 'newer' and the previously existing Haversian system. (For more information on image acquisition, see Fig. 1; numbers on 2D images indicate slice numbers; scale bar: 100 µm).

*Type 1: lateral branching*

The first type of branching observed in human cortical bone is lateral branching. It is characterized by a smaller osteon

issuing out from a larger osteon (Fig. 3). The smaller branch often abruptly juts out from the larger osteon, on occasion even adopting a perpendicular lateral course for a few

hundred microns before it proceeds longitudinally and unilaterally through adjacent tissue. The cross-sectional shape and Haversian canal orientation of the relatively larger Haversian system often remains relatively unchanged, whereas the smaller osteon begins with a much smaller diameter and gradually achieves full size as it proceeds. This indicates that the larger osteon is older and that its Haversian canal was likely the site for the branch's activation and progression.

*Type 2: dichotomous branching*

As suggested by Stout et al. (1999), osteonal structures that appear 'dumbbell-like' in cross-section represent sections through branching events, specifically of the type described here as dichotomous (Fig. 4). Close to the location of dichotomous branching, typically both the osteonal segment and its canal show 'dumbbell-' or 'figure eight'-shaped contours, gradually further separating. The two branches resulting from dichotomous branching are usually of similar size subsequent to the branching event; however,

either one or both may enlarge as it issues on its unidirectional path. The fact that all involved elements undergo structural changes close to the branching site suggests that the two develop roughly simultaneously, through a bifurcation of the cutting cone.

*Type 3: branching morphology of Haversian systems after remodeling of a previously existing system by a relatively younger system (intraosteonal remodeling)*

Haversian systems growing within the boundaries of another Haversian system were frequently observed within the current sample. The 'internal' systems were usually not well centered within the remains of the previously existing canal, but instead off-centered, and the course of the two systems could spatially diverge from each other, resulting in a branching event. In some cases the 'internal' osteon continuously occupied another Haversian system along the entire reconstructed volume. However, in far more frequent cases, this type of remodeling was discontinuous in the following ways: (i) the internal Haversian system began with a

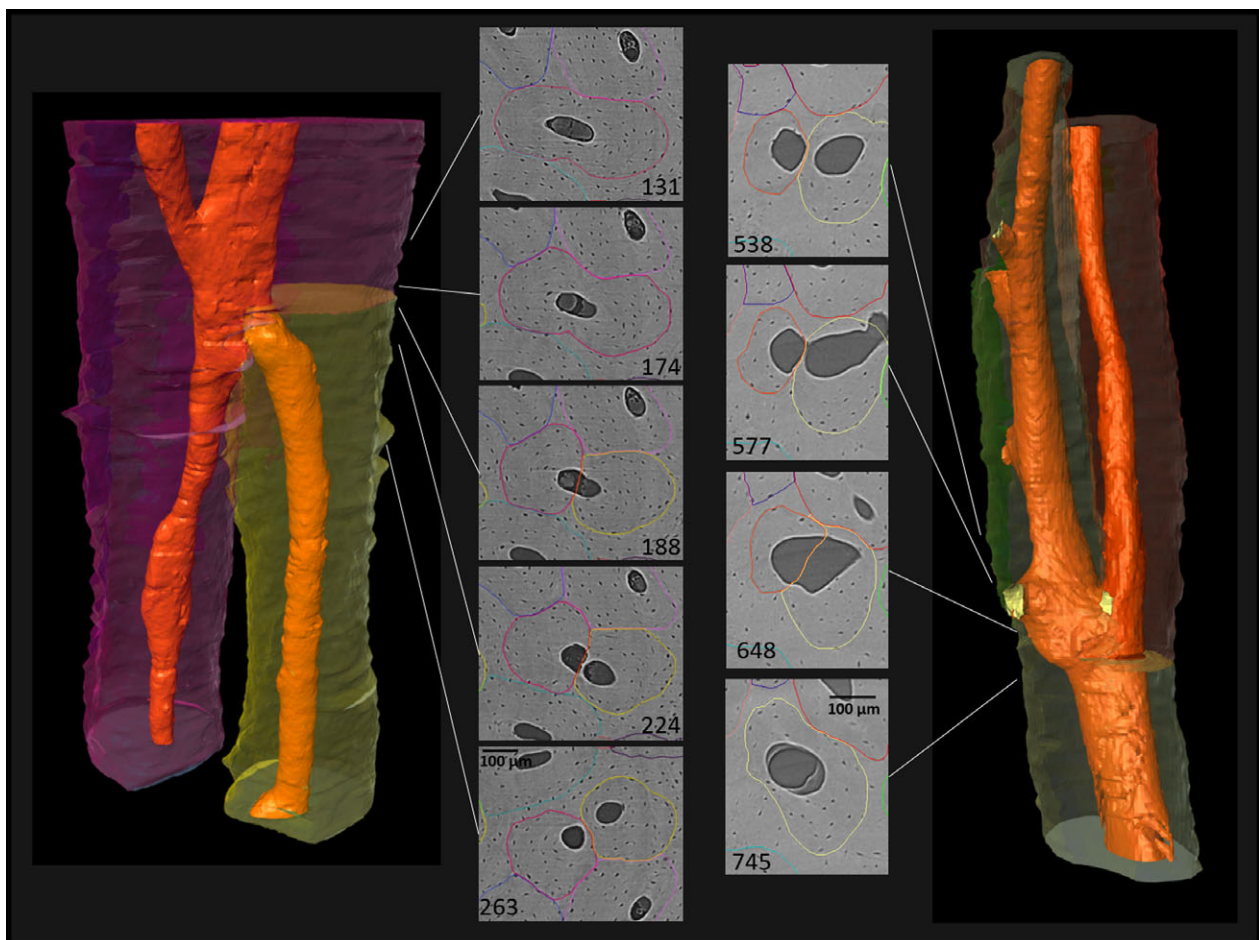


**Fig. 4** Dichotomous branching resulting in two osteonal branches of similar size. Note the structural changes of the original Haversian system in the cross-sectional view before bifurcation ('dumbbell-shape'), suggesting a simultaneous development of both branches. (For more information on image acquisition, see Fig. 1; numbers on 2D images indicate slice numbers; scale bar: 100 µm).

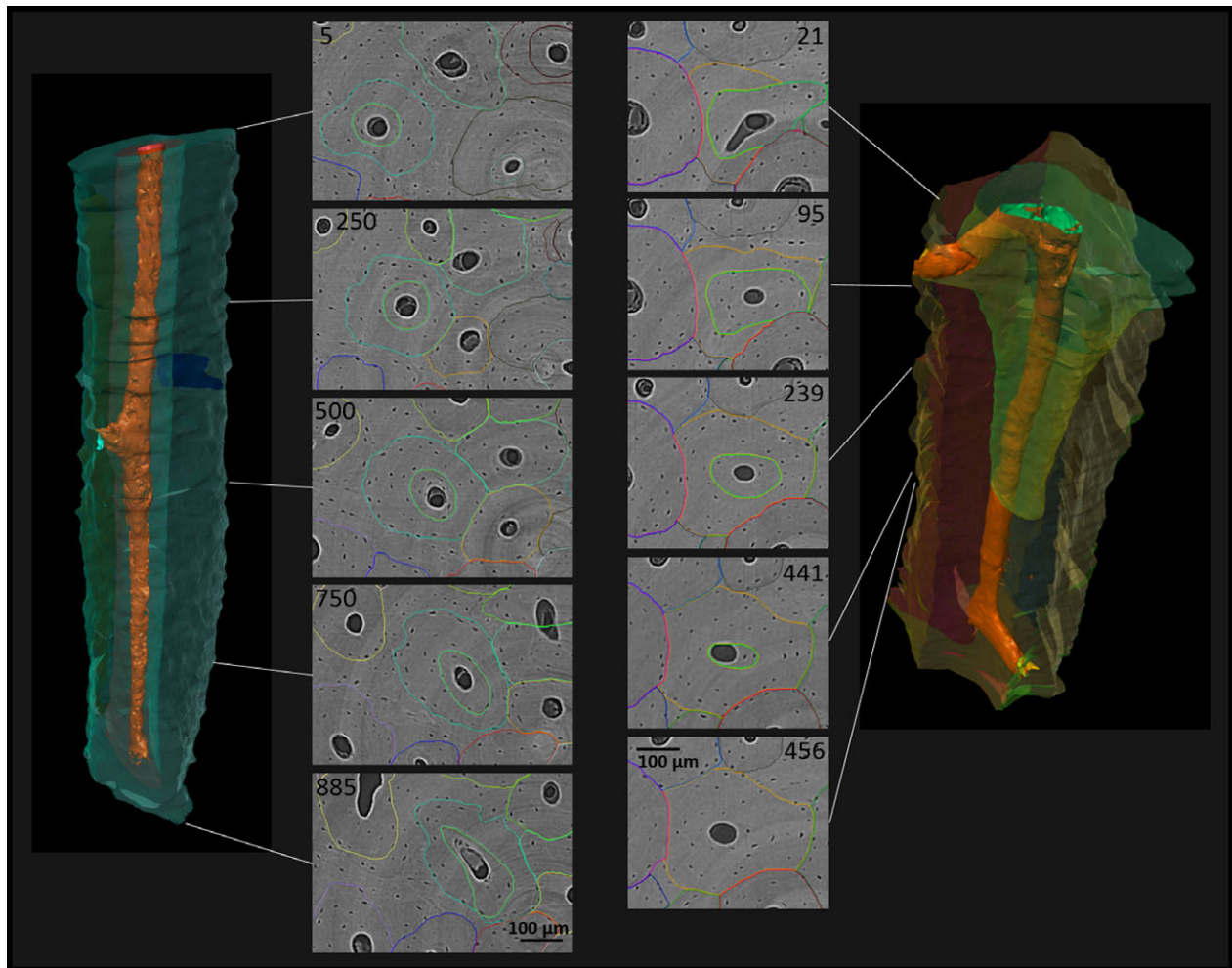


**Fig. 5** Remodeling of previously existing Haversian systems by relatively younger systems. Left: Haversian system progressing through a previously existing Haversian system throughout the sampled volume. Note the acentric reversal line of the younger osteon in cross-sectional view, when compared with the outer contour of the previously existing osteon. Right: a younger Haversian system (green) grows within the volume of a previously existing Haversian system (yellow) and increasingly narrows its cross-section around the yellow system's Haversian canal before it discontinues. (For more information on image acquisition, see Fig. 1; numbers on 2D images indicate slice numbers; scale bar: 100  $\mu\text{m}$ ).

small diameter around the previously existing Haversian canal, expanded substantially and then disappeared out of the rendered volume without exiting the original cement line (Fig. 5); or (ii) more frequently, the internal Haversian system spatially diverged from the previously existing Haversian system, breaking through its cement line with its own and creating a true branching event (Fig. 6).

### The 3D diversity of transverse connections

To separate transverse connections from branching events, all connections were defined where both or all osteonal segments involved showed uninterrupted Haversian canals before and after the event, as transverse connections. As lamellae were not visible in the micro-CT scans, the ability to accurately identify the origin of transverse connections was limited. Altogether, transverse connections are characterized

by a great diversity of diameter and course, from linear to non-linear. For example, they can be gently sloped or strongly oblique, even curved; and in many cases their course gives some clues about their origin (Figs 7 and 8).

### Quantitative analysis of branching and transverse connections

According to the observations, three categories of interconnections between Haversian systems were quantified (category 1: lateral and dichotomous branching; category 2: remodeling within previously existing Haversian systems; category 3: transverse connections). The total number of outlined osteonal segments per sample varied between 21 and 63. Haversian systems interacted with adjacent systems between zero and eight times within the 1.3 mm range included in the sample. The average total number of all

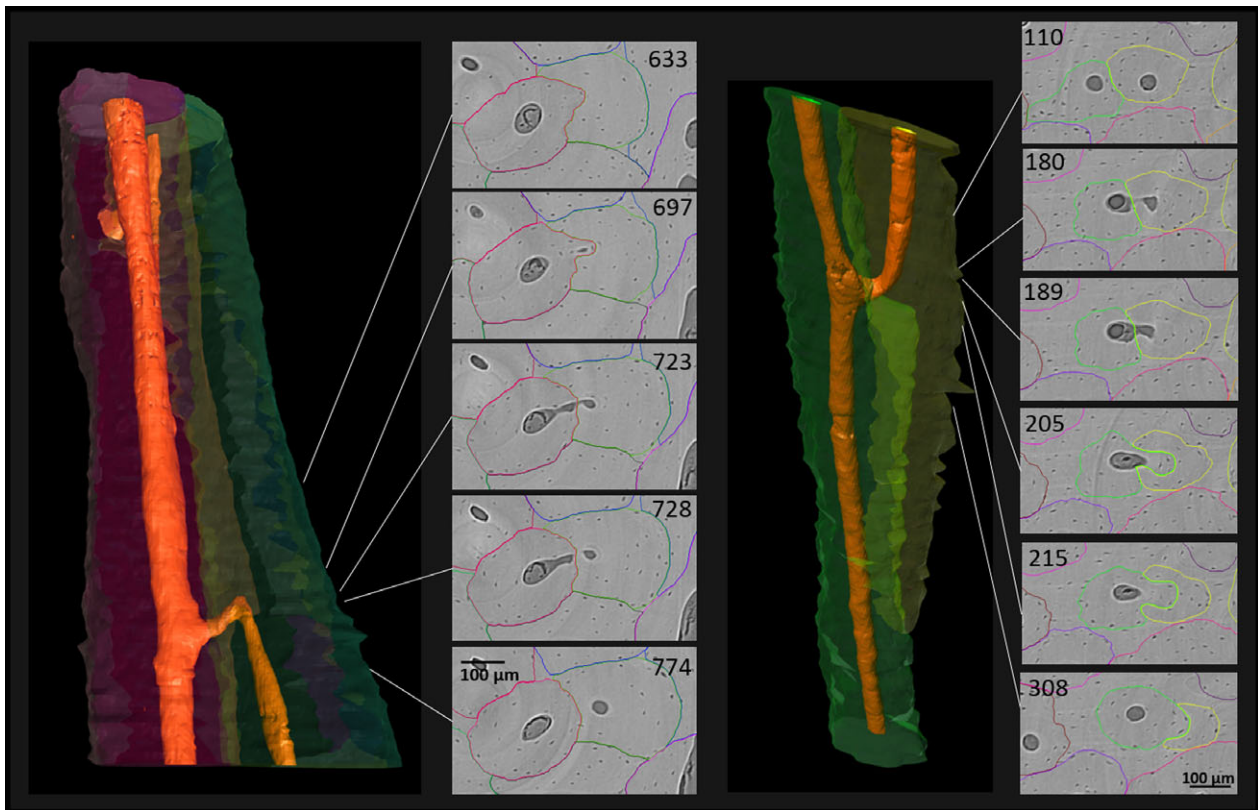


**Fig. 6** Branching morphology following relatively younger Haversian systems growing within previously existing systems. Left: the green osteonal segment has been remodeled by the red osteonal segment (from top downwards), which shifted the original canal to the left, turning over adjacent tissue (evidence for this process offers the relatively long fragment remaining of the previously existing Haversian system along the side of the younger system). Once the younger Haversian system spatially diverges far enough from the volume of the previously existing Haversian system, the younger system retains its canal (visible in the lower third of the image). Canals of both systems are connecting, most likely during formation of the younger system. Right: in this similar case, the green system is the younger system that is repathing by the yellow system. Note that in cross-section, both previously existing Haversian systems alter between being a fragment and an intact osteon along their longitudinal course. (For more information on image acquisition, see Fig. 1; numbers on 2D images indicate slice numbers; scale bar: 100  $\mu\text{m}$ ).

interconnections together per osteonal segment and per sample was between 1.59 and 2.58. Within the 1.3 mm z-axis analysed in the present study, some segments (between two and 11 per sample) connected with each other more than once, and the average number of repetitive connections between two osteonal segments was six. While the total number of osteonal segments and the total number of interconnections were higher in older individuals, with a peak in the 39 year old, there was no consistent age-related trend in the average number of interconnections per osteonal segment (Fig. 9).

Despite the consistency in the average number of interconnections per osteon across age, age-related trends were found when the frequency of the three categories of interconnections was analysed separately (Fig. 10). In the two youngest individuals (20 and 27 years), transverse connections were most common, while more evidence of intraosteonal remodeling can be found with increasing age. Lateral branching and dichotomous branching showed no consistent age-related pattern.

## Discussion

The present study shows that synchrotron radiation-based micro-CT is a valuable tool for 3D reconstructions of Haversian networks. The resolution and detail achieved in these reconstructions, with only 14.5  $\mu\text{m}$  between each hand-traced osteonal boundary, interconnected through 3-D IMAGING software, revealed the course of and interactions between Haversian systems in a degree of detail previously unachieved via imaging (see Cooper et al. 2011 for more details on the method used). As the results of the present study emphasize, total Haversian networks and remodeling mechanisms in human cortical bone are more complex than frequently appreciated.

The hand-outlining method used in this study is extremely time consuming and, as a consequence, introduces several limitations that future research will overcome. Obviously the total sample size could not be large enough to permit full statistical analysis in an exploratory study such as this. Refinement of the technique or eventual

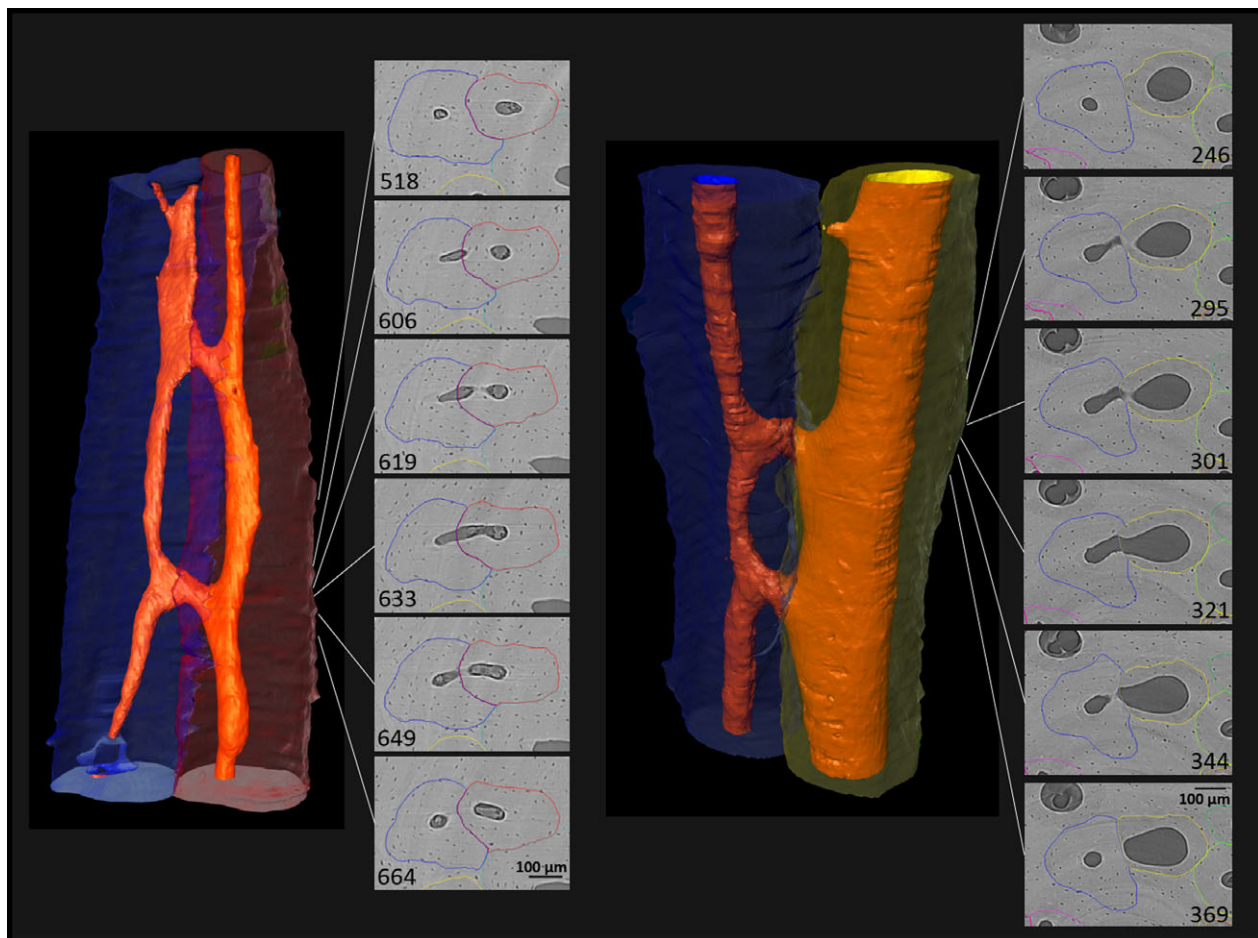


**Fig. 7** Linear transverse connections. During the development of linear transverse connections, two Haversian systems connect through short, transverse, linear canals. These connections could derive from cutting cones resorbing through tissue and creating connections with adjacent systems. It is interesting to mention that wherever these connections occur, there is a large interface between the two interacting osteons, and sometimes even some degree of overlap, pointing to the likelihood that one of the systems was repairing the other somewhere either above or below the field of view. (For more information on image acquisition, see Fig. 1; numbers on 2D images indicate slice numbers; scale bar: 100 µm).

auto-recognition of cement lines would greatly increase the usable sample size and permit broader analysis. Likewise, in order to collect data from individuals of different sexes and ages, the longitudinal depth of the resolved tissue was limited, which will also be improved by refinements of the method and technology with continued research. As it is, the reconstructed z-axis is relatively short when compared with previous measurements of the distance between branching nodes and length measurements of Haversian systems. For example, Filogamo (1946) reported a maximum length for Haversian systems of 9.6 mm in younger individuals and 7 mm in adults. Cooper et al. (2006) reported a maximum range of resorption cavities at about 5.4 mm with a mean at about 2.7 mm, leading to their suggestion that Haversian systems could be up to 6 mm or longer. Johnson (1964) also suggested resorption cavities could be up to 10 mm long. Additionally, it has been reported that osteonal segments do not usually continue for more than 3 mm without branching (Koltze, 1951). Beddoe (1977) reported

an average distance between canal intersections of 2.5 mm. Many osteonal segments were continuous throughout the entire z-axis, restricting the ability to see how Haversian systems begin and end. Koltze (1951), for example, who reconstructed regionally diverse samples of diaphyseal human bone from one individual, described how Haversian canals connect to void spaces in spongy bone towards the epiphysis. Even without complete observation, however, it seems likely that in some cortices, osteons end in large resorptive bays on the inner cortex (Maggiano, 2012). This is even evidenced in macroscopic observation of the medullary cavity, which has numerous large ridges and curved valleys running longitudinally, the likely result of endosteal resorption opening each of these long bays. Accordingly, Cohen & Harris (1958) noticed a periosteal to endosteal course of Haversian systems in their 3D reconstruction. Future work should detail possible activation or termination nodes for osteons.

Another way for an osteon to discontinue transpires within the mid-cortex itself through relatively rare

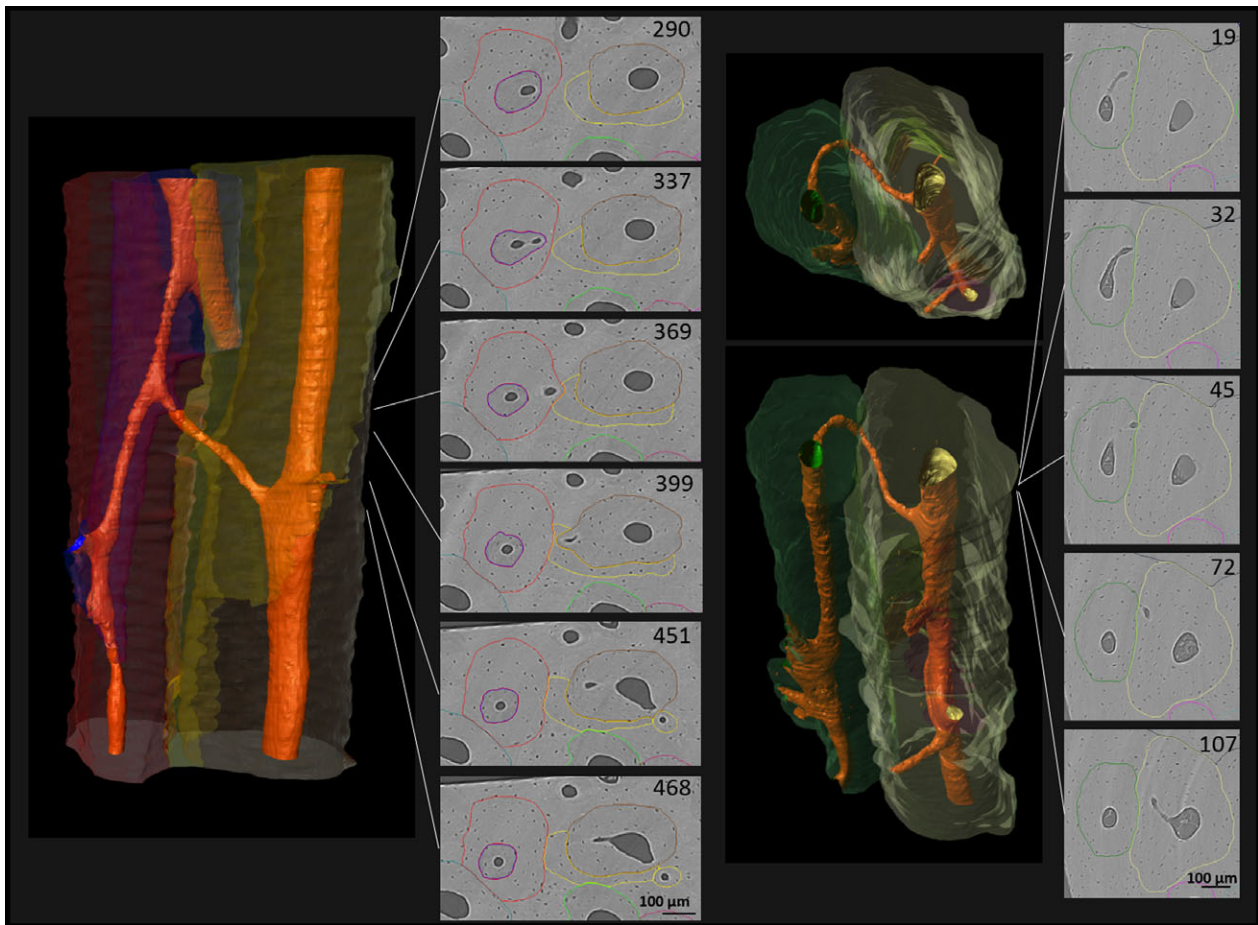


**Fig. 8** Non-linear transverse connections. Left: oblique connection (typically best viewed from the plane parallel to the osteon course). Right: curved and oblique connection (curves are especially visible when using the orthogonal plane). These relatively thin canals have likely ‘tunneled’ through existing osteonal tissue as evidenced by the relatively unchanged shape and size of both Haversian canals in the vicinity of the transverse connection. Note that in both cases, due to the canals’ oblique courses, in any given 2D slice, they are only visible as small holes. (For more information on image acquisition, see Fig. 1; numbers on 2D images indicate slice numbers; scale bar: 100 µm).

occurrences called ‘blind’ or sealed osteons (Koltze, 1951; Cohen & Harris, 1958; Congiu & Pazzaglia, 2011). In three dimensions, blind osteons gradually become narrower before they end. Their canal closes in short distance to the closure of their surrounding lamellae. This distinguishes them from actively forming Haversian systems, which toward their closing cone typically show circumferences similar to mature Haversian systems (Cooper et al. 2006). Studies suggest diverse reasons for the occurrence of blind osteons, as for example a relationship to necrotic vessels making them evidence for the dynamic requirements of intracortical blood flow (Schumacher, 1935; Koltze, 1951; Cohen & Harris, 1958; Congiu & Pazzaglia, 2011) and/or trauma (Henrie et al. 2014). Henrie et al.’s (2014) suggestion is interesting as only one of the individuals in this study had a noticeably high prevalence of blind osteons within the sample volume (seven vs. either zero or one in all other individuals). Further analyses could potentially reveal important relationships between blind osteons and

the lifespans of vessels and/or histomorphological responses in bone to vascular trauma.

Beginnings and endings of Haversian systems within cortical bone remain incompletely characterized for two major reasons: (i) terminations are often simply dramatic expansions on the inner cortex called ‘resorption bays’; (ii) they seem to end by running out of the bone itself along the medullary cavity (Maggiano, 2012); and (iii) direct observation is of course challenging as time-series analysis is difficult at these magnifications in bone. However, recent studies have made some important steps toward longitudinal tracking of remodeling (Pratt et al. 2015). Despite the fact that a complete understanding of ‘beginnings’ and ‘endings’ of Haversian systems in human cortical bone is not directly evidenced by the results, the sequential z-axis imaging provided by the current technique is useful for further characterizing differences in structure depending on the origin of the remodeling event. The current observations together with previous analyses (Koltze, 1951) suggest the

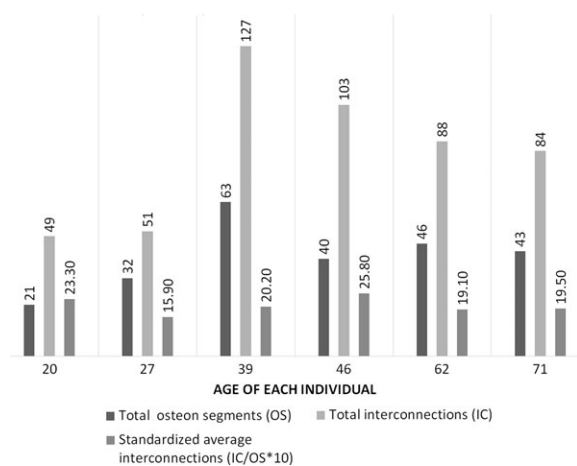


**Fig. 9** Number of osteonal segments and interconnections per individual.

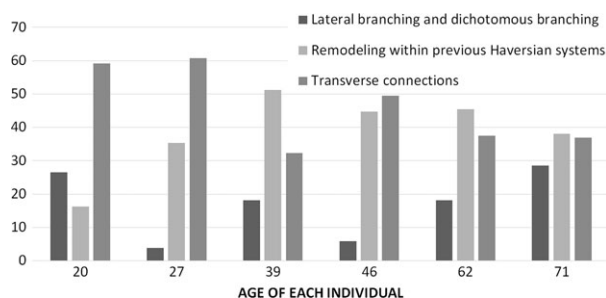


**Fig. 10** Frequency of lateral and dichotomous branching, remodeling within previously existing Haversian systems, and transverse connections. (Total numbers standardized by the total number of interconnections per sample.)

beginnings and endings of Haversian systems can either be extra-osteonal or intra-osteonal. Extra-osteonal activation starts at primary canals or the surface of trabecular voids and results in 'type I' osteons. As all of the samples were extracted from mid-cortical bone, these sites could not be observed in the present study but have been addressed elsewhere (Koltze, 1951). Intra-osteonal remodeling can be found at two different locations, according to the current results: (i) at branching nodes; and (ii) on the surface of previously existing Haversian canals, creating type II osteons in cross-section.

Another limitation common to many investigations of the Haversian network is how difficult it is to determine directionality of a given osteonal segment if the entire Haversian system either is not visible in the reconstructed volume or has ambiguous morphology. Although this study does not supply a solution for this difficulty, in some cases the gentle slope of a branching event combined with its internal osteonal origin seems to be good evidence indicating directionality. Despite the benefits of the current study's consideration of reversal line morphology, understanding

total Haversian microstructure is still challenging due to several factors. The first is that multiple scales of structure are in play in remodeled human cortical bone: (i) the total Haversian network, the net amalgamation of all Haversian systems in a region or element; (ii) the osteonal segment, or Haversian system; (iii) the canal network, which can include non-Haversian systems like primary osteons or primary canals; (iv) the vascular network, which in a single Haversian canal for example could theoretically house multiple vessels and/or vessel branches or anastomoses; (v) and finally, the microporous structure of the lacuno-canalicular system itself. Some of these challenges may be met by future advances, such as improved resolution, which could enable the viewing of lamellar structure. That said, a potentially more potent approach may be combining several histological techniques in combined studies using transverse and longitudinal light, confocal, scanning electron and 3D microscopies when possible, creating a broader picture. Pazzaglia et al. (2012), for example, used scanning electron microscopy to show that lamellae in human Haversian systems are not always circular and concentric, but often spiral and crescent-moon-shaped. The orientation of these 'partial-lamellae' could inform on osteonal drift or other aspects of branching event morphology. Eventually the goal is to characterize the functional morphology of bone at each of these levels, including hard tissue, void space and vascular morphological variation, a grand undertaking.

The present study added the morphological analysis of reversal lines to this elusive complete picture, and was able to differentiate two different types of branching in human cortical bone: (i) lateral branching, resulting in relatively small, notably unidirectional BMUs that branch off of a larger Haversian system (Fig. 3); (ii) dichotomous branching, during which one Haversian system bifurcates into two systems of similar size (Fig. 4). Previous 3D analyses of human Haversian systems reported the occasional enlargement of osteonal cross-sections at bifurcation sites (Koltze, 1951; Cohen & Harris, 1958) and osteons developing a 'dumbbell-shape' (Stout et al. 1999) in cross-section. This can frequently be observed during dichotomous branching, during which the branching Haversian system experiences significant structural changes. These structural changes suggest that the involved branches grow simultaneously, or at least nearly so. This suggestion is also supported by previous studies reporting branch-like or cluster-like resorption cavities in human cortical bone (Bell et al. 2001; Cooper et al. 2006) and non-human animal bone (Pazzaglia et al. 2011). In contrast, during lateral branching, the relatively larger Haversian system barely changes size, shape, or their canal's size or shape, suggesting these relatively smaller systems start out tunneling themselves through the mature tissue of previously existing Haversian systems.

In addition to these two branching types, Haversian systems growing inside other Haversian systems are frequently

observed. In cross-section, these show patterns previously defined as type II osteons, resulting in the 'osteon within an osteon' microstructure (Tomes & de Morgan, 1853). These type II osteons were previously described as small and inconsequential compared with 'normal' remodeling, and were assumed to remain within the confines of their parent osteon (Jaworski et al. 1972; Ortner, 1975; Richman et al. 1979; Ericksen, 1991; Nyssen-Behets et al. 1997). Ortner (1975) argued that the internal osteons are short and narrow, and might primarily serve mineral exchange. Other authors suggested they could be related to the repair of brittle canal walls (Nyssen-Behets et al. 1997). Here, type II osteons that continue, internally, along the entire reconstructed volume (1.3 mm; Fig. 5) are reported. Arhatari et al. (2011) noted a continuous type II course of even 7.5 mm. This leads to the interesting notion that any set of canal contents can simply be reused, or 'repathed', by a younger osteon, and that the more complete picture of bone remodeling relies on this repathing to turn-over tissue in regions with sufficient vascularization. Along their longitudinal course, cross-sectional shapes and outlines of the younger osteonal segments during repathing are marked by true reversal lines and do not correspond to the reversal line of the larger, pre-existing osteon, and do not necessarily occupy a position in the center of the old osteon's diameter (sometimes occupying only one side of the previous osteon). This shows that they do not represent temporal interruptions of the infilling process of the initial cutting cone, otherwise defined as double-zonal osteons in previous studies (Pankovich et al. 1974; Ericksen, 1991).

Interestingly, these observations do not suggest much of a meaningful difference between type I and type II osteons. In fact, they raise the intriguing possibility that most, if not all, osteons with fragments result from a type II osteon either below or above the plane of sectioning, or volume of reconstruction. The observations here also suggest that type II osteons are only describable as such for a variable distance before the relatively younger, internal system crosses the reversal line of the previously existing system, characteristic for the third type of branching observed here; branching following repathing (Fig. 6). During this type of branching, previously existing Haversian systems, which turned into fragments by a repathing system, quite often have their canal (and potentially their vessel) 'returned to them' by a transverse canal (Fig. 6). The latter is likely made possible by an angiogenic event supplying the younger Haversian system with its own vessel system. This occurrence encourages the realization that fragments in human cortical bone can often be current rather than historic remodeling features. Some previous 3D reconstructions by Koltze (1951) and Cohen & Harris (1958) noted that Haversian systems could become fragments and then appear as intact Haversian systems again in other tissue depths, but neither investigation included a more detailed description nor an explanation of how

this could affect the vascular system and the continuity of canals and vessels.

The continuity of Haversian systems within human cortical bone and the fact that terminal nodes are rarely seen also suggests that remodeling is often bilaterally oriented. Tappen (1977) described resorption cavities traveling in both longitudinal directions, distal and proximal, as 'paired'. The author quantified the morphology of resorption cavities in dog bones and found that between 34% and 42% of all resorption cavities were paired. However, he suggested his counts were underestimations, as many cavities extended beyond his tissue blocks, and also noted the presence of paired resorptive cavities in human bone (Tappen, 1977). A more recent study from vanOers et al. (2008) employed computer simulations showing that paired Haversian systems are the result of the strain environment around the cavity. Pazzaglia et al. (2011) note that the bidirectionality of the overall network could be a benefit for plastic alteration of blood flow direction dependent on needs of the tissue. It is important to consider these concepts for the activation and progression of 'type II' osteons, as they, too, could also frequently be 'paired', initiating somewhere along the Haversian canal and progressing in both directions. If this is the case, the internal osteon narrowing around the canal of its host Haversian system (Fig. 5) could theoretically represent the terminal completion of such an event. Still, the frequency and morphology of lateral and dichotomous branches indicates that unidirectional osteonal pathing is also common, and that this morphology is also consistent with the beginning of unidirectional repathing.

In addition to remodeling form and directionality, the current study also has implications for understanding interconnectivity in human secondary bone microstructure. In previous literature, three different kinds of transverse connections were reported in human cortical bone: (i) extensions of Haversian canals forming as the cutting cone 'swings around' and creates transverse connections with neighboring systems (Tappen, 1977); (ii) 'breakout zones', the points of initiation of BMU activity (Tappen, 1977); and (iii) canals created by 'perforating', 'penetrating' or 'tunneling' through existing tissue (Pommer, 1927; Jaffe, 1929; Schumacher, 1935). 'Tunneling' canals are usually referred to as Volkmann canals (Volkmann, 1863), Volkmann, however, originally described vascular canals forming during osteomyelitis, and the comparability of his observations with normal, healthy human bone has been put in question (Cooper et al. 1966). Extensions of Haversian canals are characterized by a surrounding lamellar structure as they are incorporated into the Haversian system during formation (Cohen & Harris, 1958). The same structural pattern can be expected in 'breakout zones', although in mature systems these two types of transverse connections cannot be differentiated morphologically. In contrast, tunneling canals are known to have no surrounding lamellae (Jaffe, 1929). As mentioned in the Results section, it was not possible to

view lamellae; however, the presence or absence of a reversal line and other important aspects of the connected systems' transverse tunnel and Haversian canal morphology can be noted, greatly benefiting examination of transverse canals in bone.

Another encouraging area for future research is the statistical analysis of the qualitative age-related trends observed in this study. Despite relative consistency in the total number of interconnections per osteonal segment, the frequency of specific types of interconnections appears age related. Lateral and dichotomous branching show diverse frequencies across all ages, but are the least frequent in the individual age 27 years, which showed larger volumes of primary lamellar bone within the sample. As studies on regional tissue variation in human and non-human primate cortical bone show, even when a standardized region is sampled, variability in drift magnitude and remodeling rates can cause tissue to have variable ages and origins (McFarlin et al. 2008; Goldman et al. 2009; Maggiano, 2015; Maggiano et al. 2015). Numerous studies have also drawn attention to regional variation of osteon properties caused by different strain environments (Hert et al. 1994; Iwaniec et al. 1998; Chan et al. 2007; Skedros et al. 2007).

Evidence for remodeling of previously existing Haversian systems by relatively younger systems increases with age, and these kinds of connections seem to replace transverse connections, which show a decrease in frequency. Transverse connections, specifically tunneling connections, might be more necessary in younger individuals as osteonal networks have not reached the same degree of complexity and interconnectivity as in older individuals. In this context, Cohen & Harris (1958) suggested an interesting relationship between the origin of remodeling events and the distance between osteocytes and blood vessels, leading to a general rule of thumb that a canal in bone is necessary roughly every 600  $\mu\text{m}$ . What happens in bone remodeling during the need to achieve this requirement in development is likely quite different than what transpires after maturation to maintain it. In general, there is a lack of knowledge translation and theoretical integrity between bone vasculature and the remodeling process that limits the ability to interpret 3D visualizations of human Haversian networks. Despite the implication in many seminal works that every remodeling event contains an extending blood vessel that grows as the BMU progresses (Frost, 1966), the current exploratory observations, specifically the observations regarding Haversian systems growing within previously existing Haversian systems, during which existing vessels are most likely being reused, suggest this may not be the case. Supporting this, Brookes & Revell (1998) note that this is not known to be mandatory – even the mere association of nearby existing vascular mesenchyme might be sufficient to supply the remodeling effort with necessary cellular recruitment and nutrient supply, a concept echoed by Parfitt (1994). Direct observation of Haversian vasculature is rare,

specifically in human bone, due to understandable limitations on studies of living specimen. Pazzaglia et al. (2007, 2011) used multiplanar analysis and a dyeing method to study the vascular system of rabbits. Their results not only emphasize an unexpected variability in vessel course, from 'blind-ended' to 'short-radius-bend' vessels to 'button-hole' figures, but also the capability of the vascular system to adapt to changing blood-flow requirements. The rarity of references addressing the number or type of vessels occupying osteonal canals in human cortical bone (Cooper et al. 1966) is evidence that much more study is necessary to further identify the relationship between BMU activity, blood vessels, anastomoses and/or angiogenesis. Though the current project does not directly observe vascular structure, its attempt to understand the sequence of events generating particular sets of interacting Haversian systems in human cortical bone points us in a productive direction by directly observing osteonal morphology in addition to the canal network.

## Acknowledgements

The authors are grateful to the mortuary staff and the staff of the Donor Tissue Bank of the Victorian Institute of Forensic Medicine for their assistance in the collection of this series of bone specimens. The authors are particularly grateful to the next-of-kin of the donors for permission to remove bone for research purposes. This research used resources of the Advanced Photon Source, a US Department of Energy (DOE) Office of Science User Facility operated for the DOE Office of Science by Argonne National Laboratory under Contract No. DE-AC02-06CH11357. Funding for this research came from the Canada Research Chairs program and the Canadian Foundation for Innovation.

## References

- Arhatari BD, Cooper DML, Thomas CDL, et al. (2011) Imaging the 3D structure of secondary osteons in human cortical bone using phase-retrieval tomography. *Phys Med Biol* **56**, 5265–5274.
- Basillais A, Chappard C, Bensamoun S, et al. (2004) Three-dimensional characterization of cortical bone porosity on microcomputed tomography images: a new method of evaluation. *J Bone Miner Res* **19**, S112–S113.
- Beddoe AH (1977) Measurements of the microscopic structure of cortical bone. *Phys Med Biol* **22**, 298–308.
- Bell KL, Loveridge N, Reeve J, et al. (2001) Super-osteons (remodeling clusters) in the cortex of the femoral shaft: influence of age and gender. *Anat Rec* **264**, 378–386.
- Britz HM, Jokihaara J, Leppänen OV, et al. (2012) The effects of immobilization on vascular canal orientation in rat cortical bone. *J Anat* **220**, 67–76.
- Brookes M, Revell WJ (1998) *Blood Supply of Bone*. London: Springer.
- Burr DB (1993) Remodelling and the repair of fatigue damage. *Calcif Tiss Int* **53**(Suppl 1), S75–S81.
- Carter Y, Thomas CD, Clement JG, et al. (2013) Femoral osteocyte lacunar density, volume and morphology in women across the lifespan. *J Struct Biol* **183**, 519–526.

- Carter Y, Suchorab JL, Thomas CDL, et al. (2014) Normal variation in cortical osteocyte lacunar parameters in healthy young males. *J Anat* **225**, 328–336.
- Chan AHW, Crowder CM, Rogers TL (2007) Variation in cortical bone histology within the human femur and its impact on estimating age at death. *Am J Phys Anthropol* **132**, 80–88.
- Cohen J, Harris WH (1958) The three-dimensional anatomy of haversian systems. *J Bone Joint Surg*, **40-A**, 419–434.
- Congiu T, Pazzaglia UE (2011) The sealed osteons of cortical diaphyseal bone. Early observations revisited with scanning electron microscopy. *Anat Rec* **294**, 193–198.
- Cooper RR, Milgram JW, Robinson RA (1966) Morphology of the osteon. *J Bone Joint Surg* **48-A**, 1239–1271.
- Cooper DML, Turinsky AL, Sensen CW, et al. (2003) Quantitative 3D analysis of the canal network in cortical bone by micro-computed tomography. *Anat Rec* **274B**, 169–179.
- Cooper DML, Matyas JR, Katzenberg MA, et al. (2004) Comparison of microcomputed tomographic and microradiographic measurements of cortical bone porosity. *Calcif Tissue Int* **74**, 437–447.
- Cooper DML, Thomas CDL, Clement JC, et al. (2006) Three-dimensional microcomputed tomography imaging of basic multicellular unit-related resorption spaces in human cortical bone. *Anat Rec* **288A**, 806–816.
- Cooper DML, Erickson B, Peele A, et al. (2011) Visualization of 3D osteon morphology by synchrotron radiation micro-CT. *J Anat* **219**, 481–489.
- Enlow DH (1963) *Principles of Bone Remodeling*. Springfield, IL: Charles C. Thomas.
- Erickson MF (1991) Histologic estimation of age at death using the anterior cortex of the femur. *Am J Phys Anthropol* **84**, 113–228.
- Filogamo G (1946) La forme et la taille des osteones chez quelques Mammiferes. *Arch Biol* **57**, 137–143.
- Frost HM (1963) *Bone Remodeling Dynamics*. Springfield, IL: Thomas.
- Frost HM (1966) *The Bone Dynamics in Osteoporosis and Osteomalacia*. Springfield, IL: Thomas.
- Frost HM (1969) Tetracycline-based histological analysis of bone remodeling. *Calcif Tissue Res* **3**, 211–237.
- Goldman HM, McFarlin SC, Cooper DMI, et al. (2009) Ontogenetic patterning of cortical bone microstructure and geometry at the human mid-shaft femur. *Anat Rec* **292**, 24–64.
- Hennig C, Thomas CD, Clement JG, et al. (2015) Does 3D orientation account for variation in osteon morphology assessed by 2D histology? *J Anat* **227**, 497–505.
- Henrie TR, Dalton M, Skedros JG (2014) Sealed osteons: a pathological consequence or natural circumstance of extensive remodeling? *Am J Phys Anthropol* **153**, 140.
- Hert J, Fiala P, Petrtyl M (1994) Osteon orientation of the diaphysis of the long bones in man. *Bone* **15**, 269–277.
- Iwaniec UT, Crenshaw TD, Schoeninger MJ, et al. (1998) Methods for improving the efficiency of estimating total osteon density in the human anterior mid-diaphyseal femur. *Am J Phys Anthropol* **107**, 13–24.
- Jaffe HL (1929) The vessel canals in normal and pathological bone. *Am J Pathol* **5**, 323–332.
- Jaworski ZF, Meunier P, Frost HM (1972) Observations on two types of resorption cavities in human lamellar cortical bone. *Clin Orthop* **83**, 279–285.
- Johnson LC (1964) Morphological analysis of pathology. In: *Bone Biodynamics* (ed. Frost HM), pp. 543–654. Boston: Little Brown.
- Kerley ER (1965) The microscopic determination of age in human bone. *Am J Phys Anthropol* **23**, 149–163.
- Koltze H (1951) Studie zur ausseren Form der Osteone. *Z Anat Entwicklungsgesch* **115**, 584–596.
- Maggiano CM (2012) Making the mold: a microstructural perspective on bone modeling during growth and mechanical adaptation. In: *Hard Tissue Histology: an Anthropological Perspective*. (eds Stout S, Crowder C), pp. 45–90. Boca Raton: CRC Press.
- Maggiano CM (2015) Methods and theory in bone modeling drift: comparing spatial analyses of primary bone distributions in the human humerus. *J Anat* **228**(1), 190–202.
- Maggiano IS, Maggiano CM, Tiesler V, et al. (2011) A distinct region of microarchitectural variation in femoral compact bone: histomorphology of the endosteal lamellar pocket. *Int J Osteoarch* **21**, 743–750.
- Maggiano IS, Maggiano CM, Tiesler VG, et al. (2015) Drifting diaphyses: asymmetry in diametric growth and adaptation along the humeral and femoral length. *Anat Rec* **289**(10), 1689–1699.
- Martin RB (2002) Is all cortical bone remodeling initiated by microdamage? *Bone* **30**, 8–13.
- Martin RB (2007) Targeted bone remodeling involved BMU steering as well as activation. *Bone* **40**, 1574–1580.
- Martin RB, Burr DB, Sharkey NA (1998) *Skeletal Tissue Mechanics*. New York: Springer.
- Matsumoto T, Yoshino M, Asano T, et al. (2005) Monochromatic synchrotron radiation  $\mu$ CT reveals disuse-mediated canal network rarefaction in cortical bone of growing rat tibiae. *J Appl Physiol* **100**, 274–280.
- McFarlin SC, Terranova CJ, Zihlman AL, et al. (2008) Regional variability in secondary remodeling within long bone cortices of catarrhine primates: the influence of bone growth history. *J Anat* **213**, 308–324.
- Nyssen-Behets C, Duchesne PY, Dhém A (1997) Structural changes with aging in cortical bone of the human tibia. *Gerontology* **43**, 3116–3325.
- van Oers RFM, Ruimerman R, vanRietbergen B, et al. (2008) Relating osteon diameter to strain. *Bone* **43**, 476–482.
- Ortner DJ (1975) Aging effects on osteon remodeling. *Calcif Tissue Res* **18**, 27–36.
- Pankovich AM, Simmons DJ, Kulkarni VV (1974) Zonal osteons in cortical bone. *Curr Orthop Pract* **100**, 356–363.
- Parfitt AM (1994) Osteonal and hemi-osteonal remodeling: the spatial and temporal framework for signal traffic in adult human bone. *J Cell Biochem* **55**, 273–286.
- Parfitt AM (2002) Targeted and nontargeted bone remodeling: relationship to basic multicellular unit origination and progression. *Bone* **30**, 5–7.
- Pazzaglia UE, Bonaspetti G, Rodella LF, et al. (2007) Design, morphometry and development of the secondary osteonal system in the femoral shaft of the rabbit. *J Anat* **211**, 303–312.
- Pazzaglia UE, Congiu T, Marchese M, et al. (2011) Structural pattern and functional correlations of the long bone diaphyses intracortical vascular system. Investigation carried out with China ink perfusion and multiplanar analysis in the rabbit femur. *Microvasc Res* **82**, 58–64.
- Pazzaglia UE, Congiu T, Marchese M, et al. (2012) Morphology and patterns of lamellar bone in human Haversian systems. *Anat Rec* **295**, 1421–1429.
- Pazzaglia UE, Congiu C, Pienazza A, et al. (2013) Morphometric analysis of osteonal architecture in bones from healthy young

- human male subjects using scanning electron microscopy. *J Anat* **223**, 242–254.
- Pommer G** (1927) Ueber den Begriff und Bedeutung der durchbohrenden Knochenkanäle. *Z Mikrosk Anat Forsch* **9**, 540–584.
- Pratt IV, Belev G, Zhu N** (2015) In vivo imaging of rat cortical bone porosity by synchrotron phase contrast micro computed tomography. *Phys Med Biol* **60**(1), 221–232.
- Richman EA, Ortner DJ, Schuller-Ellis FP** (1979) Differences in intracortical bone remodeling in three aboriginal American populations: possible dietary factors. *Calif Tiss Int* **28**, 209–214.
- Schaffler MB, Choi K, Milgrom C** (1995) Aging and matrix micro-damage accumulation in human compact bone. *Bone* **17**, 521–525.
- Schneider P, Stauber M, Voide R, et al.** (2007) Ultrastructural properties in cortical bone vary greatly in two inbred strains of mice as assessed by synchrotron light based micro- and nano-CT. *J Bone Miner Res* **22**, 1557–1570.
- Schultz M** (2001) Paleohistopathology of bone: a new approach to the study of ancient diseases. *Am J Phys Anthropol* **116**, 106–147.
- Schumacher S** (1935) Zur Anordnung der Gefäßkanäle in der Diaphyse langer Röhrenknochen des Menschen. *Z Mikrosk Anat Forsch* **38**, 145–160.
- Skedros JG, Holmes JL, Vajda EG, et al.** (2005) Cement lines of secondary osteons in human bone are not mineral-deficient: new data in a historical perspective. *Anat Rec A Discov Mol Cell Evol Biol* **286A**, 781–803.
- Skedros JG, Sorenson SM, Jenson NH** (2007) Are distributions of secondary osteon variants useful for interpreting load history in mammalian bones? *Cells Tissues Organs* **185**, 285–307.
- Stout SD** (1988) The use of histomorphology to estimate age. *J Forensic Sci* **33**, 121–125.
- Stout SD, Brunsden BS, Hildebolt CF, et al.** (1999) Computer-assisted 3D reconstruction of serial sections of cortical bone to determine the 3D structure of osteons. *Calcif Tissue Int* **65**, 280–284.
- Tappen NC** (1977) Three-dimensional studies on resorption spaces and developing osteons. *Am J Anat* **149**, 301–317.
- Tomes J, de Morgan C** (1853) Observations on the structure and development of bone. *Philos Trans R Soc Lond B Biol Sci* **143**, 109–139.
- Vasciaveo F, Bartoli E** (1961) Vascular channels and resorption cavities in the long bone cortex the bovine bone. *Acta Anat* **47**, 1–33.
- Volkman R** (1863) Zur Histologie der Karies und Ostitis. *Arch f Klin Chir*, iv, 437.